Kapal: Jurnal Ilmu Pengetahuan dan Teknologi Kelautan
(Kapal: Journal of Marine Science and Technology)
journal homepage : http://ejournal.undip.ac.id/index.php/kapal
2301-9069 (e)
1829-8370 (p)

Effect of Pitch Distribution on The Propeller Efficiency and Cavitation of Offshore Patrol Vessels 98 Meter

Novan Risnawan[1)*], Taufiq Arif Setyanto[2)], Erzi Agson Gani[1)], Mahendra Indiaryanto[2)], Berlian Arswendo Adietya[3)]

[1)]Indonesia Defence University, Republic of Indonesia, Bogor - Indonesia
[2)]Research Center for Hydrodynamics Technology, National Research and Innovation Agency (BRIN), Surabaya - Indonesia
[3)]Department of Naval Architecture, Universitas Diponegoro, Semarang-Indonesia
[*)]Corresponding Author: nova006@brin.go.id

Article Info

Keywords:
Propeller;
Cavitation;
Pitch Distribution;
CFD;
Burril Diagram;

Article history:
Received: 08/12/2024
Last revised: 08/05/2025
Accepted: 29/05/2025
Available online: 29/05/2025
Published: 30/06/2025

DOI:
https://doi.org/10.14710/kapal.v22i2.68808

Abstract

This paper discusses the effect of pitch distribution on the propeller of a high-speed vessel (Offshore Patrol Vessel) on propeller efficiency and cavitation on the propeller blade surface. A propeller model design with five blades featuring symmetric blade contours and ogival-shaped foil, tested through open water tests in a towing tank, is used as the research object. Three variations of pitch distribution based on PropCAD recommendations: original pitch, 80% hub pitch distribution, and high-thrust pitch distribution, are used as parameters to calculate propeller efficiency using Computational Fluid Dynamics (CFD). The cavitation phenomena occurring on the propeller blades under each pitch distribution condition are analysed using the Burrill method (Burrill Diagram). Based on CFD analysis, it was found that the propeller with the highest propeller efficiency, η, is obtained from the high-thrust pitch distribution (0.6072), compared to the original pitch distribution (0.5902) and the 80% hub pitch distribution (0.5651). Cavitation occurs in all three pitch variations because the thrust loading coefficient values (τ_c) for the original pitch distribution (0.1286), 80% hub pitch distribution (0.1183), and high-thrust pitch distribution (0.1293) are higher than the cavitation threshold from the Burrill diagram ($\tau'_c = 0.0783$).

Copyright © 2025 KAPAL: Jurnal Ilmu Pengetahuan dan Teknologi Kelautan. This is an open access article under the CC BY-SA license (https://creativecommons.org/licenses/by-sa/4.0/).

1. Introduction

The Indonesian Navy's 98-meter Offshore Patrol Vessel has a length of 98 meters, a width of 13.50 meters, and a height of 6.90 meters. This vessel can be operated as both a patrol ship and a warship. It has a maximum speed of 28 knots and a cruising speed of 20 knots. This speed performance is achieved through a propulsion system with five blades, 3850 mm diameter, and a NACA 16 Mod profile type propeller as the main propulsion component, which is the original profile used in the propeller series model [1] [2].

The propeller converts mechanical energy from the engine into thrust. It plays a crucial role in determining a vessel's manoeuvrability, especially for high-speed vessels like Offshore Patrol Vessels. Therefore, optimising propeller performance, involving a combination of thrust parameters, propeller efficiency, and cavitation phenomena, has become a key focus for marine propeller engineers and the subject of numerous studies [3]. Ship propellers are designed with the aim of achieving optimal performance while also considering the effects of cavitation phenomena [4].

Research on improving propeller performance has also been conducted by modifying the camber ratio of the propeller blade foil [5], where the propeller was designed with symmetric blade shapes and ogival Foil. Additionally, studies have been carried out to analyse changes in propeller performance by modifying the shape of the propeller blade foil using numerical simulations with Computational Fluid Dynamics (CFD) [6].

Furthermore, a study conducted by Boucetta & Imine [7] and Mahendra et al. [8] Demonstrated that using Ogival Foil on propeller blades can effectively reduce drag caused by the interaction between the propeller blades and fluid flow. On the other hand, the study conducted by B. A. Adietya et al. [9] aimed to improve propeller performance by adding a cap fin and a duct. Research by [10] Provided additional insights into the impact of pitch distribution variations on cavitation, which directly affects propeller performance. However, to date, no specific research has addressed the influence of pitch distribution on the efficiency and cavitation of high-speed vessel propellers. However, specific research focused on the influence of pitch distribution on the efficiency and cavitation of high-speed vessel propellers still needs to be further explored.

With the background above, this paper discusses the influence of pitch distribution on the efficiency and cavitation of high-speed vessel propellers, specifically the OPV 98-meter. The research utilises a propeller model with a diameter of 146 mm, featuring five blades with a symmetrical blade contour and ogival-shaped foil. The propeller model was experimentally tested (open water test) at the towing tank facility of the Hydrodynamics Laboratory - BRIN. Three pitch distribution variations were applied: original pitch, 80 hub pitch distribution, and high-thrust pitch distribution. Propeller efficiency differences were analysed using Computational Fluid Dynamics (CFD), while cavitation phenomena under the three pitch distribution conditions were analysed using the Burrill Diagram.

2. Method

To obtain the efficiency values of the propeller model under three pitch distribution conditions, original pitch distribution, 80% hub pitch distribution, and high-thrust pitch distribution, calculations were performed using Computational Fluid Dynamics (CFD) to determine K_T, K_Q, and efficiency (η). Meanwhile, cavitation calculations were conducted using the Burrill Diagram approach. The propeller model used as the research object is a high-speed vessel (OPV 98 M) propeller model with symmetric blade shapes and ogival foil.

2.1. Modelling

The object of this research is a propeller with symmetric blade contours using Ogival Foil, designed for high-speed vessels (OPV 98 m). This study aims to analyse the performance of the propeller based on pitch distribution modifications and their effect on cavitation phenomena using the Burrill Diagram. The propeller model used in this research is specified in Table 1 and illustrated in Figure 1.

Table 1. Specifications of the high-speed vessel (OPV 98 M) propeller model.

Dimension	Notation	Value
Diameter Model Propeller	D	146 m
Pitch Diameter Ratio	P/D	143.1
Blade Area Ratio	BAR	1.182
Number of blades	Z	5
Nominal Pitch	P	20892.6 m

Figure 1. High-speed vessel (OPV 98 M) propeller model

2.2. Governing Equation

The partial differential equations describing fluid behavior are used to analyze the turbulent flow behavior around a propeller model. The RANSE continuity and momentum equations are used to model fluid flow, including laminar and turbulent flow, in the context of CFD) and propeller analysis [11]. The basic RANSE (continuity equation) can be formulated in Eq. 1 and 2 with the momentum equations can be written in tensor notation and Cartesian coordinates [12]:

$$\frac{\partial U_i}{\partial x_i} = 0 \tag{1}$$

$$\frac{\partial U_i}{\partial t} + U_j \frac{\partial U_i}{\partial_{xj}} = -\frac{1}{\rho}\frac{\partial P}{\partial x_j} + \frac{\partial}{\partial x_j}\left[\mu\left(\frac{\partial U_i}{\partial x_j} + \frac{\partial U_j}{\partial x_i}\right)\right] - \frac{\overline{\partial u_i' u_j'}}{\partial x_j} \tag{2}$$

Where ρ is the density of the fluid, U_i is the average component of the flow velocity in the i direction, x_i is the coordinate in the i direction, μ is the dynamic viscosity, ui is the fluctuation of the flow velocity in the i direction. Determining an appropriate turbulence model is an essential step in RANS simulation. $\frac{\overline{\partial u_i' u_j'}}{\partial x_j}$. The Reynolds stress modelling is defined as Explicit Algebraic.

2.3. Mesh Generation and Boundary Conditions

Figure 2 illustrates the computational domain designed in a cylindrical shape with specific boundary condition settings. The right side of the domain is defined as the velocity inlet, the left side as the pressure outlet, the cylindrical surface as the symmetry plane, and the propeller surface as a solid surface (wall boundary). In Figure 3, the velocity inlet and pressure outlet positions are placed sufficiently far from the propeller centre, which are 2D and 6D, respectively (where D is the propeller diameter). The computational domain dimensions are designed with a height and width of 6D each to ensure adequate spatial coverage for the simulation analysis [2].

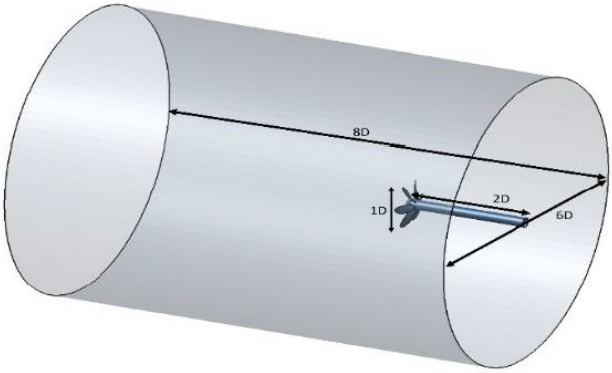

Figure 2. Computational Domain.

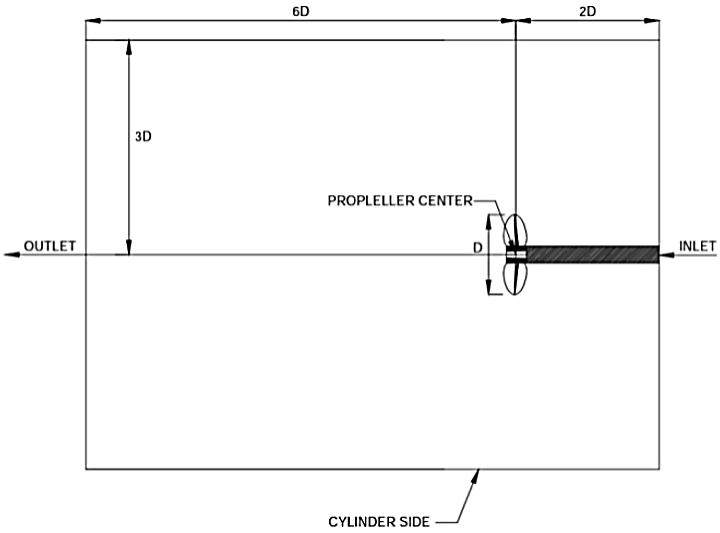

Figure 3. Boundary conditions.

Figure 4 shows the structured mesh pattern. Structured mesh provides stable and precise simulation results around the propeller [13]. Finer grids are created to capture flow details such as pressure distribution, wake, and cavitation potential [14].

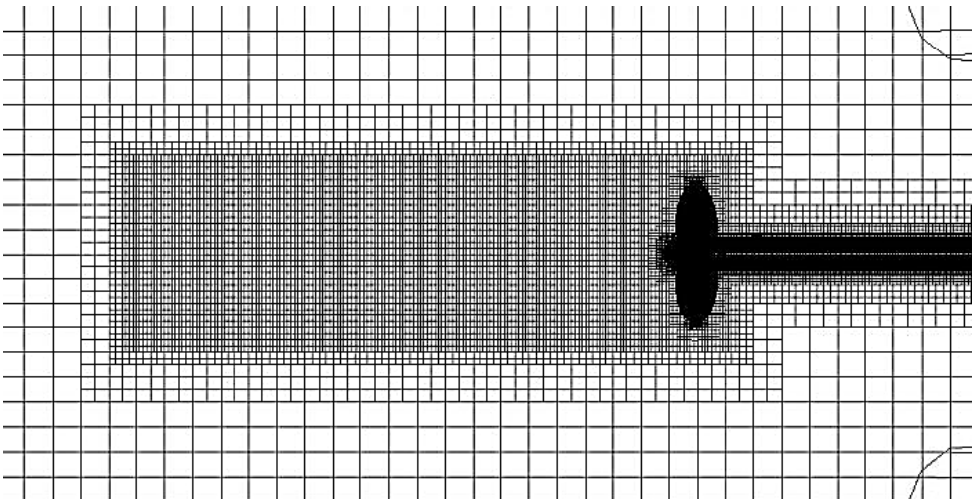

Figure 4. Structured mesh.

2.4. Grid Independence Test

Mesh quality is crucial for achieving stable simulations, with smaller or denser elements applied to areas with high gradients around the propeller blades [15]. A Grid Independence Test is a process to ensure that the simulation results do not depend on the size or density of the grid used [16]. The goal is to ensure that the numerical solution has reached convergence and does not change significantly when the number of grid elements is increased. The Grid Independence Test ensures that the simulation results remain stable regardless of the grid density used. It is performed by creating multiple grids with different levels of refinement and running the same simulation on each grid [10].

In this study, three variations of grid density were performed while maintaining a constant propeller rotational speed (1206 rpm) and the same flow velocity (Vs = 2.939 m/s). The grid generation process used coarse, medium, and delicate density levels. The purpose of these variations was to evaluate the impact of grid density on the simulation results and ensure that the obtained solution does not depend on the size or thickness of the grid used. This is important to achieve accurate simulation results with optimal computational efficiency [6].

Table 2. Grid independence of symmetrical blade contour

No	Nb	J	VS	T	Q	KT	KQ	Eff
1	517663	1.0	2.939	48.3143	1.9795	0.263192	0.073858	0.567431
2	1378094	1.0	2.939	46.9371	1.968	0.255689	0.073429	0.554478
3	2191248	1.0	2.939	47.7314	1.9776	0.260016	0.073787	0.561124

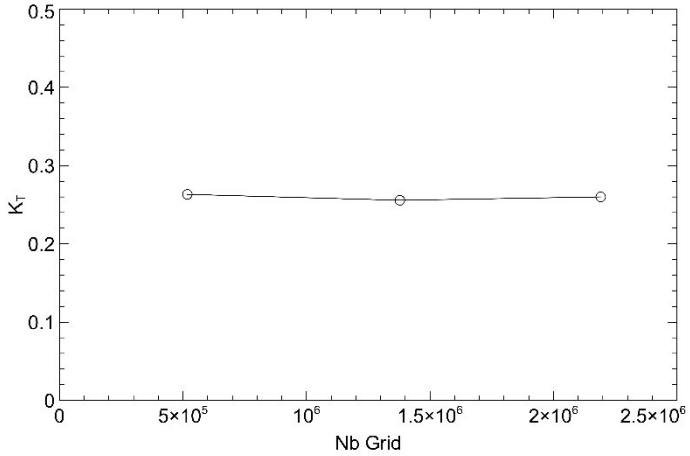

Figure 5. Grid-independent simulation of symmetrical blade contour for K_T

Table 2 shows the simulation results for three different grid densities. In the table, the change in K_T is relatively small across the three grid density variations (517,663, 1,378,094, and 2,191,248), indicating that the differences in grid density are approaching convergence (grid independence). Figure 5 shows a graph of the K_T values with the three grid independence variations, where the line shows almost no change. When the number of grid elements increased from 517,663 to 2,191,248, the change in KT values was not significant, and increasing grid density did not lead to significant changes in the simulation results [6]. Based on these results, the grid with 1,378,094 elements can be considered sufficient, providing results nearly identical to those obtained with a finer grid (2,191,248). The coarser grid (517,663) shows a slight deviation but still falls within an acceptable range. Computational efficiency can be optimised by selecting a grid density that is not too large but still provides convergent results, 1,378,094.

2.5. Pitch Distribution of Propeller

An essential parameter in propeller design is pitch distribution, which refers to the pitch angle variation along the propeller blade from the hub to the blade tip. Pitch distribution determines how the fluid flow interacts with the propeller blades at each point along the blade [14]. In Figure 6, pitch is the axial distance travelled by the propeller in one complete revolution (360 degrees). In propeller analysis, point P, which moves on the cylindrical surface with radius r, forms a helix when rotating with an angle φ. When the angle φ reaches 360° or 2π radians, the helix completes one full revolution, returning to the X–Z plane at a distance p along the OX axis from the starting point, which is formulated as $\theta = tan^{-1}(\frac{p}{2\pi r})$ [7].

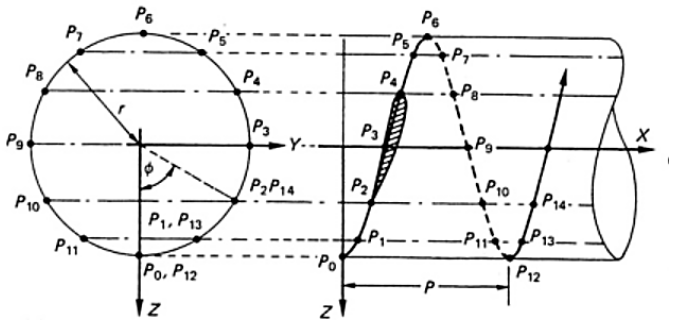

Figure 6. Pitch definition

2.5.1. Original Pitch Distribution

The original pitch distribution was derived from the original design of the high-speed vessel (OPV 98M) propeller model. Figure 7 shows the design of the propeller model for the high-speed boat (OPV 98M), where the pitch value is 208.926, evenly distributed from the root to the tip of the propeller blade.

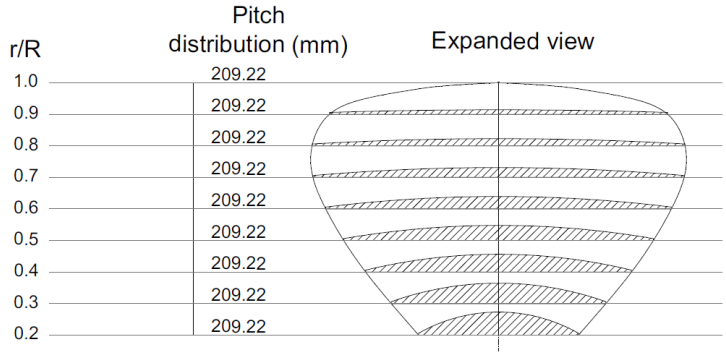

Figure 7. Propeller model with original pitch distribution.

2.5.2. 80% Hub Pitch Distribution

Pitch distribution variations were carried out based on the PropCad reference [17], specifically the 80% hub distribution and high-thrust pitch distribution. Figure 8 illustrates the 80% hub distribution, where pitch distribution modifications focus on the propeller blade section with r/R 0.2. This means the pitch angle is primarily altered near the hub area. At the same time, the blade tip section r/R 0.5 is kept more stable to maintain flow efficiency across the propeller, which is a critical zone for generating thrust and propeller efficiency.

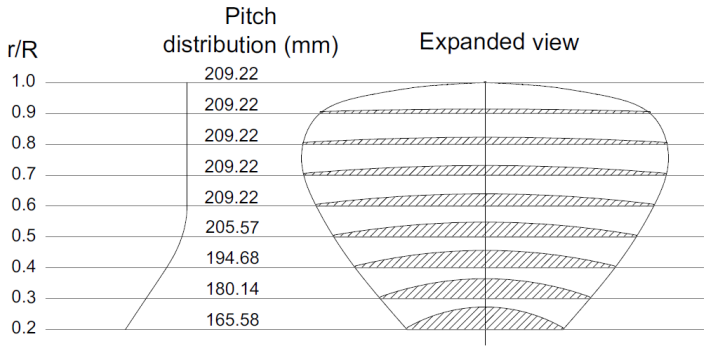

Figure 8. Propeller model with 80% Hub Pitch Distribution.

2.5.3. High-thrust Pitch Distribution

The high-thrust pitch distribution of the propeller model shown in Figure 9, based on [17], specifically optimises the pitch distribution in the 70% to 90% area (the middle to the tip section of the propeller blade: $r/R \geq 0.7$ to $r/R \geq 0.9$) to achieve maximum thrust.

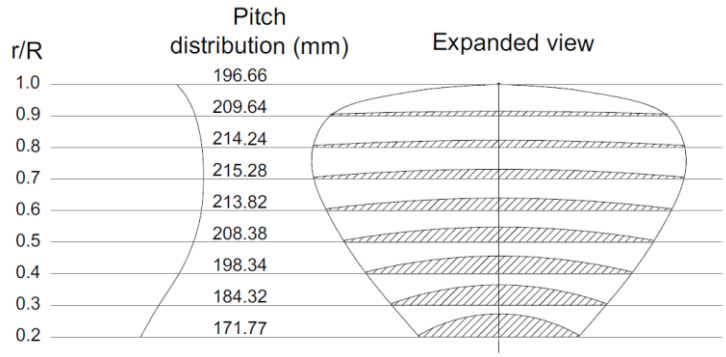

Figure 9. Propeller model with high-thrust pitch distribution.

2.5.4. Propellers Performance

Propeller performance is expressed in non-dimensional terms using parameters such as the advance coefficient (J), thrust coefficient (K_T), torque coefficient (K_Q), and efficiency (η) [2]. These characteristics are general and fully applicable to a specific geometric configuration of a propeller. Each propeller has a unique performance curve, making its characteristics specific and not generalisable to all types of high-speed vessels [6].

$$J = \frac{V_a}{nD} \tag{3}$$

$$K_T = \frac{T}{\rho n^2 D^4} \tag{4}$$

$$K_Q = \frac{Q}{\rho n^2 D^5} \tag{5}$$

$$\eta = \frac{JK_T}{2\pi K_Q} = \frac{TV_a}{2\pi nQ} \tag{6}$$

where:

J	:	Advance Coefficient
K_T	:	Thrust Coefficient
K_Q	:	Torque Coefficient
η	:	Propeller Efficiency
Q	:	Propeller Torque (Nm)
T	:	Propeller Thrust (N)
$CapV_a$	:	Advance Fluid Velocity (m/s)
n	:	Propeller Rotation (RPS)
D	:	Propeller Diameter (m)
ρ	:	Fluid Density (Kg/m^3)

2.5.5. Burill Diagram

The Burrill Diagram is used to predict the effects of cavitation on propeller blades. This diagram defines the safe operational limits of a propeller to prevent cavitation, which can damage the blades and reduce efficiency. Figure 10 illustrates the Burrill Diagram, where the x-axis represents the mean cavitation number ($\sigma_{0.7R}$), and the y-axis represents the thrust loading coefficient (τ_C).

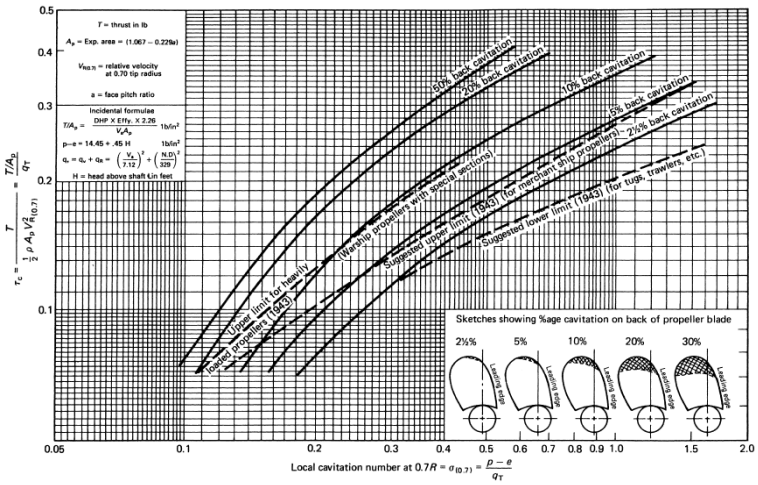

Figure 10. Burrill cavitation diagram

The cavitation calculation for the propeller is aimed at comparing the thrust loading coefficient, τ_C (Warship Propeller) between the result of the calculation, τ_C and the Burill diagram τ_C'. Furthermore, cavitation can be calculated at the 0.7R position using the cavitation number, V_R, corresponding to the initial design conditions. The formulation for the cavitation value is expressed as follows:

$$V_R^2 = \sqrt{V_A^2 + 0.7\, n\, \pi\, D^2} \tag{7}$$

The V_R value represents the relative velocity measured at the 0.7R position (70% of the propeller radius), while V_A is the advance velocity (speed of advance). Meanwhile, n denotes the propeller's rotational speed measured in rpm (rotations per second), and D is the propeller diameter.

The formulation for the cavitation value is expressed as follows:

$$\sigma_{0.7\,R} = \frac{p-e}{q_v+q_R} = \frac{14.45+0.45\,H}{\left(\frac{V_a}{7.12}\right)^2+\left(\frac{nD}{329}\right)^2} \tag{8}$$

From the cavitation number, the thrust loading coefficient τ_CIs as follows:

$$\tau_C = \frac{T/A_P}{(0.5)\rho V_R^2} \tag{9}$$

The occurrence of cavitation phenomena is determined by the relationship between the mean cavitation number and the thrust loading coefficient as follows:

τc > τc' = Cavitation occurs
τc < τc' = Cavitation does not occur

3. Results and Discussion

Table 3 presents the results of numerical calculations of propeller performance using CFD for the high-speed vessel (OPV 98M) propeller model under the conditions of original pitch, 80% hub distribution, and high-thrust pitch distribution. The simulations were conducted at the vessel's operational speed with an advanced coefficient, J = 1.0. Using Eq. 3 to 6, the values of K_Q, K_T, and η were obtained, as shown in Table 3 for each pitch condition.

Table 3. Numerical calculation result of propeller performance using CFD for three pitch distribution variations

J	Original Pitch			80% Hub			High thrust		
	K_T	$10K_Q$	η_0	K_T	$10K_Q$	η_0	K_T	$10K_Q$	η_0
0.1	0.7295	1.6968	0.0684	0.7161	1.6791	0.0679	0.7478	1.7525	0.0679
0.2	0.6839	1.5978	0.1362	0.6755	1.58858	0.1354	0.6959	1.6361	0.1354
0.3	0.6398	1.5028	0.2032	0.6398	1.5012	0.2035	0.6512	1.5242	0.2040
0.4	0.5906	1.3983	0.2689	0.5920	1.4045	0.2683	0.6055	1.4375	0.2681
0.5	0.5373	1.2889	0.3317	0.5411	0.1293	0.3332	0.5510	1.4375	0.2681

0.6	0.4839	1.1811	0.3912	0.4875	0.1184	0.3932	0.4971	1.2080	0.3929
0.7	0.4272	1.0542	0.4515	0.4333	0.1072	0.4502	0.4305	1.0713	0.4477
0.8	0.3714	0.9594	0.4929	0.3718	0.0947	0.5001	0.3794	0.9647	0.5008
0.9	0.3238	0.8528	0.5440	0.3052	0.0797	0.5483	0.3201	0.8224	0.5575
1	0.2723	0.7343	0.5902	0.2504	0.7053	0.5651	0.2738	1.2296	0.6072
1.1	0.2069	0.6247	0.5798	0.1711	0.0570	0.5257	0.2004	0.6373	0.5505
1.2	0.1387	0.5083	0.5214	0.1267	0.0502	0.4824	0.1356	0.4794	0.5404
1.3	0.0677	0.3943	0.3555	0.0574	0.0385	0.3085	0.0764	0.3652	0.5404

Figure 11 illustrates the propeller performance: torque coefficient (K_Q), thrust coefficient (K_T), and efficiency (η) from CFD calculations under operational speed conditions where the propeller rotation, n = 1206 rpm, is plotted as a function of J for three different pitch distribution variations: original pitch distribution, 80% hub pitch distribution, and high-thrust pitch distribution.

As shown in Figure 11 (a), the torque required for the propeller with high-thrust pitch distribution is the highest compared to the other two pitch variations. Meanwhile, in Figure 11 (b), the thrust produced by the propeller with high-thrust pitch distribution is also the highest compared to the other two, except at J values below 0.3, where the generated thrust decreases. Figure 11 (c) shows that the efficiency of all three pitch variations is relatively similar at J values below 0.8. However, at J = 1.0, the 80% hub pitch distribution achieves the highest efficiency, while the propeller with the original pitch distribution exhibits the lowest efficiency.

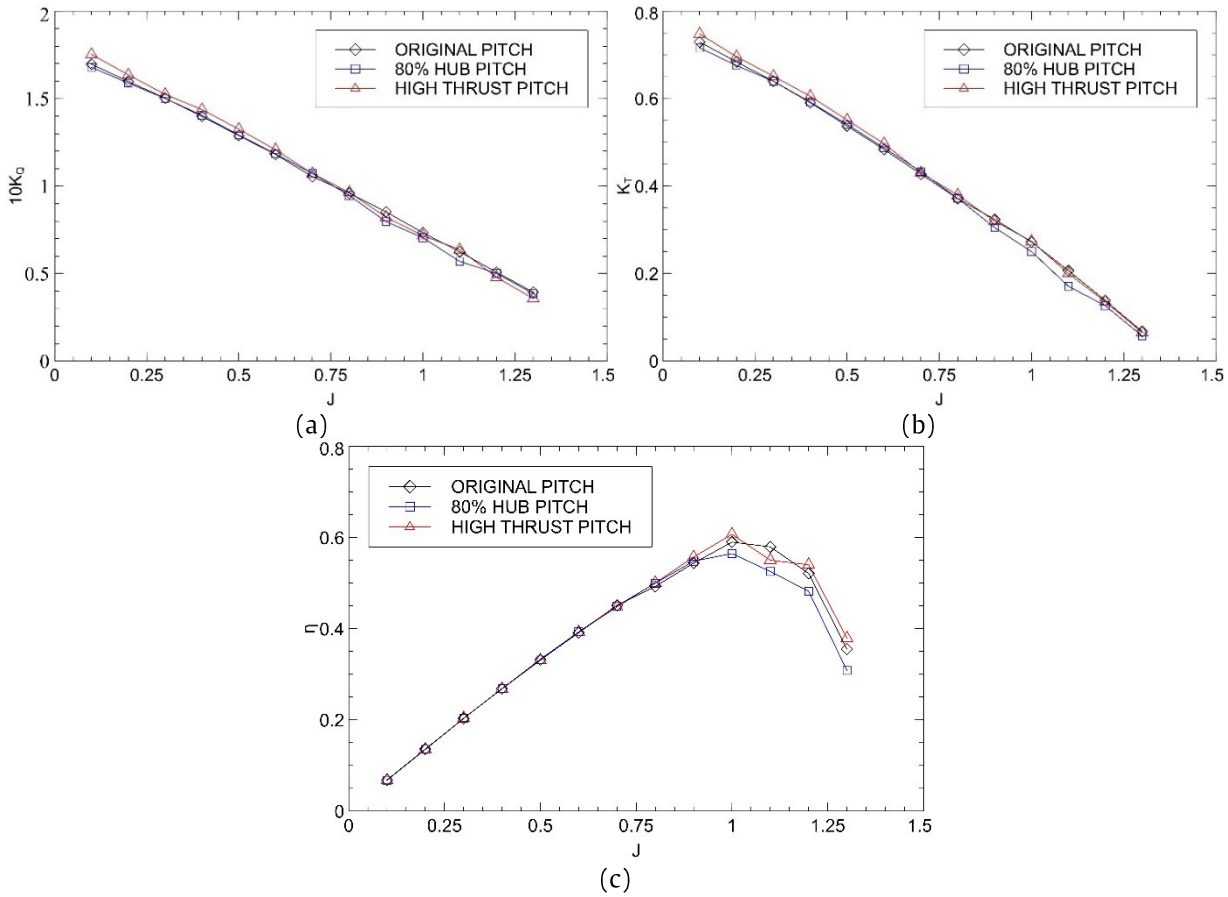

Figure 11. Comparison of propeller performance with three pitch distribution variations for (a) torque coefficient, (b) thrust coefficient, and (c) efficiency.

Table 4 shows the propeller's performance under the vessel's operational conditions at J = 1.0. The propeller achieves the highest efficiency under the vessel's operational conditions with the 80% hub pitch distribution.

Table 4. Performance of the propeller model in operational conditions when J = 1.0 (Operational Speed of Vessel)

Pitch Distribution	KT	10KQ	η
Original pitch	0.2723	0.7343	0.5902
80% hub	0.2504	0.7052	0.5651
High-thrust	0.2738	0.7175	0.6072

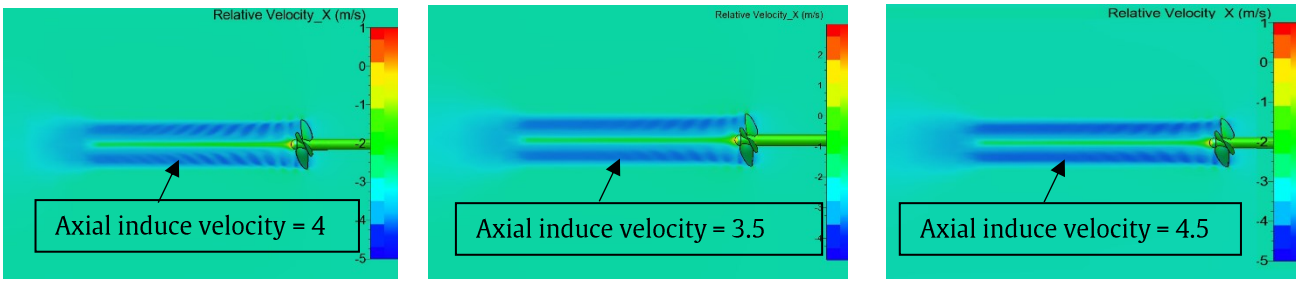

(a) (b) (c)

Figure 12. Axial induced velocity acting on the propeller for the three different pitch distributions: (a) original pitch distribution, (b) hub pitch distribution, (c) high-thrust pitch distribution

The axial-induced velocity is caused by changing the propeller rotation relative to the advance velocity. Figure 12 shows the axial induced velocity for J = 1.0. The propeller with high-thrust pitch distribution gives the highest axial induced velocity, 4.5 m/s, compared to the original four m/s and 80% hub pitch distribution, 3.4 m/s. This difference is caused by the thrust resulting from each variation of pitch distribution shown in Table 4.

After successful validation of the high-thrust propeller model through CFD simulation, the next step involved conducting open water simulations on several modified propeller configurations, as illustrated in Figure 13. This study evaluates four configurations: the original high-thrust pitch and three modified versions–Modification 1, Modification 2, and Modification 3. Each configuration features a different pitch distribution pattern, designed to optimize thrust performance and efficiency. The simulation aims to analyze the hydrodynamic characteristics of each variation by examining key parameters such as thrust coefficient (KT), torque coefficient (KQ), and advance coefficient (J), which will later serve as input for the self-propulsion test phase.

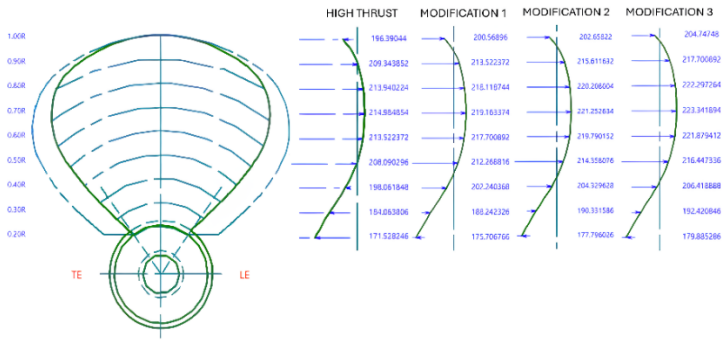

Figure 13. Distribution of the pitch propeller high thrust pitch.

Table 5 presents the numerical results of propeller performance using CFD for a high-speed vessel (OPV) propeller model modified from the high-thrust propeller design in three variations. Simulations were conducted at the vessel's operational speed with an advanced coefficient of J = 1.0. The values of K_Q, K_T, and η were calculated using Eq. 3 to 6 and are summarized in Table 5.

Table 5. CFD Results of Propeller Performance from Three Modified High-Thrust Models.

J	High thrust			High thrust (Modification 1)			High thrust (Modification 2)			High thrust (Modification 3)		
	KT	10KQ	η_0	KT	10KQ	η_0	KT	10KQ	η_0	KT	10KQ	η_0
0.1	0.7478	1.7525	0.0679	0.7778	1.8051	0.0686	0.7852	1.8402	0.0679	0.7927	1.8752	0.0673
0.2	0.6959	1.6361	0.1354	0.7237	1.6852	0.1367	0.7307	1.7179	0.1354	0.7376	1.7506	0.1341
0.3	0.6512	1.5242	0.2040	0.6773	1.5699	0.2060	0.6838	1.6004	0.2040	0.6903	1.6309	0.2021
0.4	0.6055	1.4375	0.2681	0.6297	1.4806	0.2707	0.6357	1.5094	0.2681	0.6418	1.5381	0.2656
0.5	0.5510	1.3256	0.3308	0.5730	1.3653	0.3340	0.5785	1.3918	0.3308	0.5841	1.4184	0.3277
0.6	0.4971	1.2080	0.3929	0.5169	1.2443	0.3967	0.5219	1.2684	0.3929	0.5269	1.2926	0.3892
0.7	0.4305	1.0713	0.4477	0.4477	1.1034	0.4520	0.4520	1.1248	0.4477	0.4563	1.1462	0.4435
0.8	0.3794	0.9647	0.5008	0.3946	0.9936	0.5057	0.3984	1.0129	0.5008	0.4022	1.0322	0.4961
0.9	0.3201	0.8224	0.5575	0.3329	0.8471	0.5629	0.3361	0.8635	0.5575	0.3393	0.8800	0.5523
1.0	0.2738	0.7175	0.6073	0.2848	0.7391	0.6132	0.2875	0.7534	0.6073	0.2902	0.7678	0.6016
1.1	0.2004	0.6373	0.5505	0.2084	0.6564	0.5558	0.2104	0.6692	0.5505	0.2124	0.6819	0.5453
1.2	0.1356	0.4794	0.5404	0.1411	0.4938	0.5456	0.1424	0.5033	0.5404	0.1438	0.5129	0.5353
1.3	0.0764	0.3652	0.4328	0.0794	0.3761	0.4370	0.0802	0.3834	0.4328	0.0810	0.3907	0.4288

Figure 14 presents the propeller performance in terms of torque coefficient (K_Q), thrust coefficient (K_T), and efficiency (η), based on CFD calculations under operational speed conditions with a propeller rotation speed of n = 1206 rpm. These three parameters are plotted against the advance coefficient (J) for the high-thrust pitch modification model, comparing three variations: Modification 1, Modification 2, and Modification 3.

Figure 14(a) illustrates that the torque coefficient (K_Q) consistently decreases with increasing advance coefficient (J) across all configurations. However, Modifications 1, 2, and 3 display higher K_Q values than the original pitch design, indicating a greater torque requirement. Among the three, Modification 3 exhibits the highest torque demand, suggesting increased energy input to maintain propeller rotation.

Figure 14(b) presents the relationship between the thrust coefficient (K_T) and the advance coefficient (J). All configurations exhibit a decreasing trend in K_T as J increases. Nevertheless, all three modifications produce higher KT values compared to the original pitch configuration. Modification 3 demonstrates the highest K_T, indicating that it delivers the most optimal thrust performance among the variations.

Figure 14(c) shows the propeller efficiency as a function of the advance coefficient (J). The efficiency increases with J, reaching a peak at approximately J = 1.0, before gradually declining. All three modified configurations demonstrate higher efficiency compared to the original pitch design across most of the J range. Modification 1 achieves the highest efficiency at the peak point, making it the most efficient configuration overall.

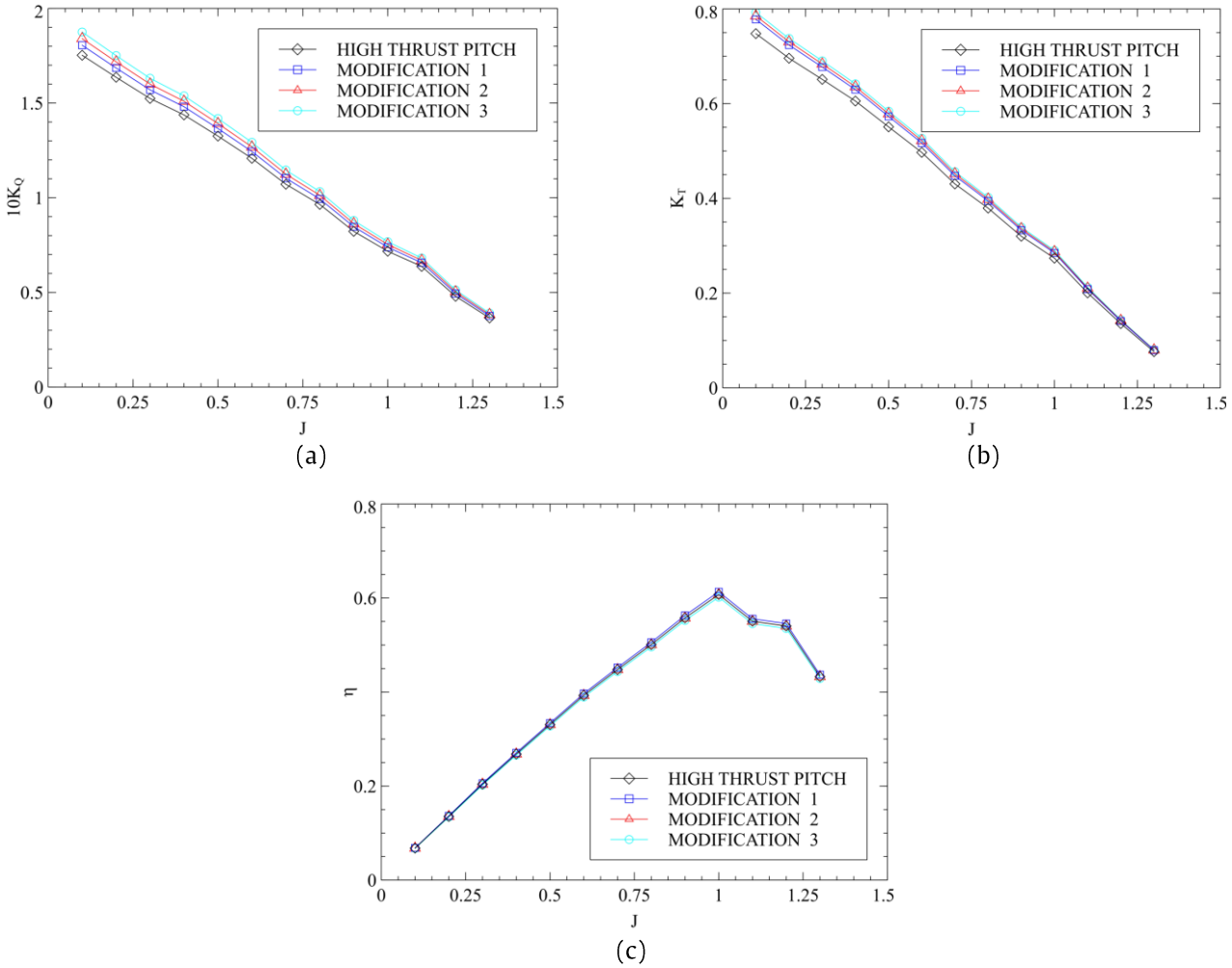

Figure 14. Comparative Performance Analysis of a High-Thrust Pitch Propeller with Three Pitch Distribution Modifications (a) torque coefficient, (b) thrust coefficient, and (c) efficiency.

3.1. Cavitation Calculation

The thrust loading coefficient τ_cIt is calculated based on Eq. 9, where the propeller thrust (T) for each pitch distribution is 11,237.6 lb, 10,333.9 lb, and 11,297.8 lb for the original pitch, 80% hub pitch, and high thrust pitch, respectively. The projected area, A_P, is 0.157 ft². The fluid flow velocity, V_R^2, relative to the propeller at the r/R = 0.7, is 133,316 ft/s², with a constant propeller rotation speed of 7577.54 rad/m and a measured propeller diameter of 0.479 ft. According to the above data, Figure 15 illustrates the cavitation calculation results using the Burrill diagram. There are three variations of cavitation calculation results for the propeller. From Eq. 7 – 9 the local cavitation values ($\sigma_{0.7R}$) obtained are 0.117 for the original pitch, hub pitch, and high-thrust pitch, respectively. Meanwhile, the thrust loading values (τ_c) They are 0.1286, 0.1183, and 0.1293 for the original, hub, and high thrust, respectively. Table 6 shows that the thrust loading value, τ_c for all three pitch variations are higher than the cavitation value of Burril τ_c'. Based on the cavitation criterion, cavitation occurs if $\tau c > \tau c'$ and cavitation does not occur if $\tau c < \tau c'$. Table 6 shows that cavitation occurs at all three pitch variations where $\tau c > \tau c'$.

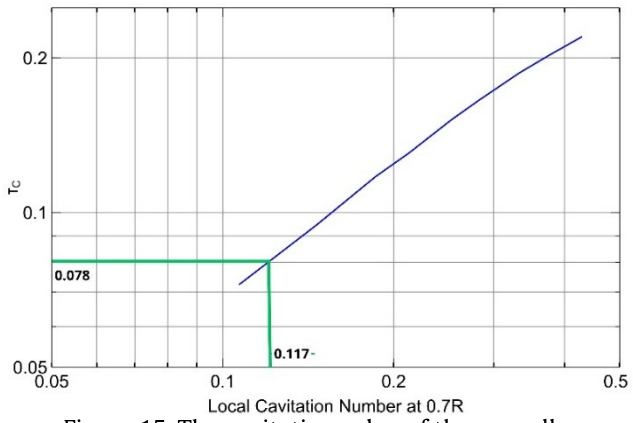

Figure 15. The cavitation value of the propeller

Table 6. Cavitation Values for Three Different Pitch Distributions when J = 1.0 (Operational Speed of Vessel)

Pitch Distribution	σ0.7R	τ_C	τ_C'	Remark
Original pitch	0.117	0.1286	0.0783	Cavitation
80% hub	0.117	0.1183	0.0783	Cavitation
High thrust	0.117	0.1293	0.0783	Cavitation

4. Conclusion

This paper examines the effect of pitch distribution variations on a propeller's performance and cavitation prediction. Three variations were selected: original pitch distribution, 80% hub pitch distribution, and high-thrust pitch distribution. The propeller performance analysis was conducted using Computational Fluid Dynamics (CFD) at a constant rpm of 1206 rpm (operational speed condition). The prediction of cavitation phenomena was analysed using the Burrill diagram for the three pitch distribution variations, where the input parameters were derived from CFD calculation results.

Based on numerical calculations, at an operational speed where the advance coefficient J=1.0 and n=1206 rpm, the highest propeller efficiency, η, is obtained from the propeller with a high-thrust pitch distribution (0.6072), compared to the original pitch distribution (0.5902) and the 80% hub pitch distribution (0.5651). Meanwhile, the prediction of the cavitation phenomenon based on the Burrill method (Burrill diagram) shows that the cavitation occurs at all three pitch variations. This is because the thrust loading coefficient values, τc for all three pitch variations, original pitch distribution (0.1286), 80% hub pitch distribution (0.1183), and high-thrust pitch distribution (0.1293) are higher than the cavitation value from the Burrill diagram (τ'_C) = 0.0783.

Acknowledgements

The first author acknowledges the Indonesia Defense University, the Republic of Indonesia, and the Ministry of Defense of the Republic of Indonesia for financial support during the study.

References

[1] G. Kuiper, The Wageningen propeller series, The Netherlands: "MARIN Publication 91-001′ Published on the occasion of its 60th anniversary, MARIN Wageningen., 1992.

[2] J. S. Carlton, Marine Propellers and Propulsion, Great Britain: Elsevier, Second edition 2007.

[3] Indiaryanto, Mahendra and I Made Ariana, "Kajian Numerik Pengembangan Symmetrical Blade Propeller Untuk Kapal Patroli 60m dengan Menggunakan Teori Lifting Line," *Rekayasa Energi Manufaktur,* vol. 2, no. 1, pp. PP. 1-5, 2017. Doi: https://doi.org/10.21070/r.e.m.v2i1.778

[4] W. Zhu, Z. Li and R. Ding, "Effect of Pitch Ratio on The Cavitation of Controllable Pitch Propeller," *Ocean Engineering,* vol. 293, no. 116692, p. PP: 17, 2024. doi: https://doi.org/10.1016/j.oceaneng.2024.116692

[5] M. D. Arifin and F. M. Felayati, "Numerical Study of Kaplan Series Propeller using CFD: Effect of Angle of Attack and Number of Blade Variations," *CFD Letters,* vol. 15, no. 8, pp. PP : 200-213, 2023. doi: http://dx.doi.org/10.12962%2Fj25481479.v5i4.8285

[6] M. Indiaryanto, K. Suastika and T. A. Setyanto, "Hydrodynamic Performance Analysis of Camber Ratio Variations on B-series Propeller Types," *CFD Letters,* vol. 16, no. 7, pp. PP. 1-15, 2024. Doi: https://doi.org/10.37934/cfdl.16.7.3953

[7] D. Boucetta and O. Imine, "CFD Analysis of Hydrofoil Flow and Cavitation," *Eng Technol Open Acc,* vol. 2, no. 5, pp. PP, 1-3, 2019

[8] M. Indiaryanto, K. Suastika and T. A. Setyanto, "Comparison of the Hydrodynamic Performance of Three Different Propeller Foil Types: NACA 66 (Mod), Ogival and NACA Symmetrical Section," *CFD Letters,* vol. 17, no. 10, pp. PP: 168-183, 2025. doi: https://doi.org/10.37934/cfdl.17.10.168183

[9] B. A. Adietya, H. Syahab, M. Indiaryanto, W. D. Aryawan and I. K. A. Pria Utama, "Influence Evaluation of Open Propellers with Boss Cap Fins: Case Studies on Types B4-70 and Ka4-70," *CFD Letters,* vol. 16, no. 9, pp. PP. 1-35, 2024. Doi: https://doi.org/10.37934/cfdl.16.9.143177

[10] X. Zhang, Qimao Xu, M. Zhang and Z. Xie, "Numerical Prediction of Cavitation Fatigue Life and Hydrodynamic Performance of Marine Propellers," *Marine Science and Engineering,* pp. PP.1-20, 2024. Doi: https://doi.org/10.3390/jmse12010074

[11] T. WATANABE, T. KAWAMURA, Y. TAKEKOSHI , M. MAEDA and S. H. RHEE, "Simulation Of Steady And Unsteady Cavitation On A Marine Propeller Using A RANS CFD Code," *Fifth International Symposium on Cavitation (CAV2003),* pp. PP : 1-8, 2003

[12] Numeca International, in *Cadence Design Systems. n.d. "FINEMarine-Theory-Guide."*

[13] A. Seeni, . P. Rajendran and H. Mamat, "A CFD Mesh Independent Solution Technique for Low Reynolds Number Propeller," *CFD Letters,* vol. 11, no. 10, pp. PP : 15-30, 2019

[14] I. E. Sandjaja, I. M. Adana, Erwandi, M. Indiaryanto, Muryadin and B. A. Adietya, "Numerical Analysis of the Effects of Propeller High Thrust Distribution on Propulsion," *Kapal:Journal of Marine Science and Technology,* vol. 3, no. 20, pp. PP. 309-319, 2023. Doi: https://doi.org/10.14710/kapal.v20i3.54715

[15] A. Mandru, L. Rusu and F. Pacuraru, "Propultion Simulation On Fully Appended Ship Model," *FASCICLE XI – SHIPBUILDING,* pp. PP. 95-100, 2021. Doi: https://doi.org/10.35219/AnnUgalShipBuilding/2021.44.14

[16] Q. Gao, W. Jin and D. Vassalos, "The Calculations of Propeller Induced Velocity by RANS and Momentum Theory," *Journal of Marine Science and Application,* vol. 11, no. 2, pp. PP : 164-168, 2012. Doi: https://doi.org/10.1007/s11804-012-1118-1

[17] HydroComp, Inc, PropCad User's Guid, Durham, NH 03824 USA: PropCad is a trademark of HydroComp, Inc., 2005

[18] S. H. Kim, Electric Motor Control, Amsterdam: Elsevier, 2017

[19] M Indiaryanto, K Suastika and T A Setyanto, "EFfect Of Chamber Ratio Variation On The Hydrodynamic Performance of the symatrical blade Type Propeller," *ICSOT Indonesia, The Royal Institution of Naval Architects, Surabaya, Indonesia,* pp. PP. 1-7, 2021.

[20] M. D. Arifin, D. Faturachman, F. Octaviani and K. A. Sulaeman, "Analysis of the Effect of Changes in Pitch Ratio and Number of Blades on Cavitation on CPP," *International Journal of Marine Engineering Innovation and Research,* vol. 5, no. 4, pp. PP. 255-264, 2020. Doi: https://doi.org/10.37934/cfdl.15.8.200213